J Therm Anal Calorim (2011) 103:485–493
DOI 10.1007/s10973-010-1081-5

Decomposition kinetic of carbonaceous materials used in a mold flux design

E. Benavidez · L. Santini · E. Brandaleze

Received: 13 April 2010 / Accepted: 30 September 2010 / Published online: 15 October 2010

Abstract Mold fluxes develop important functions during steel continuous casting process. To obtain a free-defect product the melting rate of mold flux is an important property to be controlled. The melting rate depends on the reactivity of carbonaceous material added to these powders as carbon source. In this article, the decomposition kinetic of two carbonaceous materials added to mold flux: petroleum coke and synthetic graphite, was analyzed. By measuring mass loss at different heating rates the decomposition reaction was determined on both types of materials. Applying several kinetic models of non-isothermal decomposition, the average activation energy $E = 48$ kJ/mol to mold powder with 15 wt% coke and $E = 67$ kJ/mol to one with 15 wt% graphite was determined. A first order of reaction ($n = 1$) associated to the decomposition process was assumed to both types of materials. The lower activation energy presented by mold powder-15 wt% petroleum coke indicated a higher reactivity of this material. A higher level of variation of E and n values with decomposition degree and temperature observed in the powder with petroleum coke was associated to a less thermally stable material along with a more complex degradation process.

Keywords Decomposition kinetic · Isoconversional models · Activation energy · Carbonaceous material · Mold fluxes

Introduction

Mold fluxes are used in the continuous casting (CC) of steel. The composition of these powders consists mainly of silica (SiO_2), lime (CaO), sodium oxide (Na_2O), spar (CaF_2), and carbon. The continuous casting mold fluxes are designed for specific steel grades and steel plant conditions. They must satisfy several requirements: (1) form a liquid slag pool to protect the molten steel surface from oxidation, (2) provide sufficient thermal insulation to prevent the surface of the steel from freezing, (3) absorb inclusions from the steel, (4) provide lubrication between the solidifying steel and the refrigerated mold wall, and (5) control the uniform heat transfer from the steel to the mold [1]. These powders are mixtures of different raw materials such as wollastonite, feldspars, carbonates, quartz, etc., so it is possible to use different minerals to obtain identical compositions. Besides, 2–20 wt% of a carbon source such as graphite, petroleum coke, or carbon black is added to the flux [2].

During the CC process these powders are poured on the liquid steel forming three layers (i) an unreacted powder layer on top, (ii) a carbon enriched sintered layer in the middle, and (iii) a molten flux layer in direct contact with the steel [3]. Carbon forms CO (gas) and thereby protects the steel surface from oxidation. On the other hand, the molten layer forms a liquid flux pool and then it flows into the gap between the mold wall and the solidified steel shell. The molten pool must conserve a sufficient constant level to guarantee both adequate lubrication and uniform heat

Electronic supplementary material The online version of this article (doi:10.1007/s10973-010-1081-5) contains supplementary material, which is available to authorized users.

E. Benavidez (✉) · L. Santini · E. Brandaleze
Departamento Metalurgia and DEYTEMA, Facultad Regional San Nicolás, Universidad Tecnológica Nacional, Colón 332, B2900LWH San Nicolás, Argentina
e-mail: ebenavidez@frsn.utn.edu.ar

extraction during steel solidification. The molten slag pool acts as a reservoir of liquid slag. Molten pool depth is controlled by flux melting rate and vertical heat flux produced by the casting conditions. For these reasons, to obtain a free defect product during CC of steel, an adequate mold powder must be selected or designed [4]. The main properties to be considered in the mold powder design are: the melting rate, the viscosity, and the crystallization temperature [2].

The melting rate depends on several casting parameters (such as casting speed), the flux composition (exothermic agents can increase the melting rate), the size and form of carbon particles, the free carbon content of the powder, and the type of carbon added [5]. The carbon particles are mixed with the other minerals and separate them during the fusion process. So, the higher the content of carbon is and/or the lower the particle size of carbon, the lower the melting rate is [6, 7]. From a thermodynamics point of view, to predict the melting rate it is important to know the reactivity of different carbon sources used in the mold powder design. It is known that the melting rate increases with increasing carbon reactivity [7]. The reactivity of powder can be determined by knowing the decomposition kinetic of carbonaceous material; in this way, lower activation energy should be associated to higher reactivity.

In this study, the decomposition kinetics of two carbonaceous materials: petroleum coke and synthetic graphite, added to a mold flux is studied. Thermogravimetric (TG) analysis was carried out at different heating rates on both samples. The TG data were analyzed by non-isothermal kinetic methods to obtain both the activation energy of decomposition as a function of conversion (isoconversional models) and the order of the reaction.

Theory

It is usually assumed that a solid state reaction is the product of two functions, one depending on the temperature and the other depending on the tansformated fraction:

$$\frac{d\alpha}{dt} = k(T) \cdot f(\alpha) \tag{1}$$

where α is the degree of conversion, T is the absolute temperature, and $f(\alpha)$ is the conversion function depending on the reaction model. The function $k(T)$ is the rate constant and is given by a Arrhenius equation, so that the Eq. 1 takes the following form:

$$\frac{d\alpha}{dt} = A \cdot e^{-\frac{E}{RT}} \cdot f(\alpha) \tag{2}$$

In this equation, A is the pre-exponential factor, E is the activation energy, and R is the gas constant. According to the selected model, the conversion function $f(\alpha)$ can take several forms [8, 9]. Under non-isothermal conditions, the reaction rate ($d\alpha/dt$) at any time depends on both the $f(\alpha)$, $k(T)$, and the Arrhenius parameters (A and E).

According to data obtained from the constant heating rate experiments $\beta = dT/dt = \text{const.}$, the Eq. 2 takes the form:

$$\frac{d\alpha}{dT} = \frac{A}{\beta} \cdot e^{-\frac{E}{RT}} \cdot f(\alpha) \tag{3}$$

integrating this expression up to a conversion value α:

$$\int_0^{\alpha} \frac{d\alpha}{f(\alpha)} = g(\alpha) = \frac{A}{\beta} \cdot \int_{T_0}^{T} e^{-\frac{E}{RT}} \cdot dT \tag{4}$$

Several methods were employed to determine the kinetic triplet ($f(\alpha)$, E, and A) that can be classified into (i) isoconversional (free model) and (ii) model fitting methods.

The isoconversional methods assume that for any value of α the conversion function $f(\alpha)$ does no change with the variation of the heating rate β. By this method it is possible to calculate the activation energy as a function of conversion α without assumptions about the reaction model. Several non-isothermal isoconversional methods have been used to study the decomposition kinetic of different materials [10–24].

The isoconversional models used in this study were proposed by Ozawa–Flynn–Wall [25, 26], Kissinger–Akahira–Sunose [27, 28], Kissinger [27], and Augis-Bennett [29]. These methods, applied to solid state decomposition reaction, need thermogravimetric data from experiments performed at different heating rates β.

Both the Ozawa–Flynn–Wall (OFW) and the Kissinger–Akahira–Sunose (KAS) methods measure the temperature T_α corresponding to a fixed value of the degree of conversion α; so, for different heating rates, different sets of T at different α levels are obtained.

The Ozawa–Flynn–Wall method [25, 26] is based on the Eq. 5:

$$\ln(\beta) = \ln\left(\frac{A.E}{g(\alpha).R}\right) - 5.3305 - 1.0516\frac{E}{R.T_\alpha} \tag{5}$$

Plotting of $\ln\beta$ versus $1/T_\alpha$ a straight line with slope of $-1.0516\ E/R$ is obtained by which the activation energy is calculated.

The Kissinger–Akahira–Sunose (KAS) method is based on the expression [27, 28]:

$$\ln\left(\frac{\beta}{T_\alpha^2}\right) = \ln\left(\frac{AR}{g(\alpha)E}\right) - \frac{E}{RT_\alpha} \tag{6}$$

The plot of $\ln(\beta/T_\alpha^2)$ versus $1/T_\alpha$ recorded at different heating rates gives straight lines whose slopes permit to

determine the values of the activation energy E at a particular α value.

The Kissinger and Augis-Bennett methods assume that the reaction rate reaches its maximum value at the peak temperature (T_P) of the $d\alpha/dT$ (DTG) curve. Therefore, a constant degree of conversion α is attained at T_P. Thus, they are grouped into isoconversional category. In both of these methods, a single value of E is obtained.

The Kissinger method [27] is based on the Eq. 7:

$$\ln\left(\frac{\beta}{T_P^2}\right) = -\frac{E}{RT_P} + \ln\left(\frac{AR}{E}\right) \quad (7)$$

The activation energy E can be obtained from the slope of the straight line corresponding to the plot $\ln(\beta/T_P^2)$ versus $1/T_P$.

According to the method suggested by Augis and Bennet [29]:

$$\ln\left(\frac{\beta}{T_P - T_0}\right) = -\frac{E}{RT_P} + \ln A \quad (8)$$

Where T_P and T_0 are the peak and the room temperature, respectively. The activation energy E can be obtained from the plot of $\ln[\beta/(T_P - T_0)]$ versus $1/T_P$.

To obtain the order of reaction (n), the analysis developed by Ozawa [30] was used. This model established the following equation:

$$\ln(-\ln(1-\alpha)) = \ln(A) - \frac{E}{RT} - n\ln(\beta) \quad (9)$$

Plotting $\ln(-\ln(1-\alpha))$ versus $\ln\beta$ the value of n can be determined. In this method, the α values measured at a same temperature are taken from the α versus T plots obtained at different heating rates.

Experimental

The industrial mold flux composition used in this study is detailed in Table 1. The mold powder was heated at 800 °C during 2 h for decarburization.

Two samples were prepared with the decarburizated mold flux, one adding 15 wt% of petroleum coke (sample C) and the other adding 15 wt% of synthetic graphite (sample G).

Thermogravimetric runs were carried out putting 155 ± 1 mg of the corresponding sample in alumina crucibles. The mass loss and the temperature were registered with a OHAUS DV114C microbalance and a thermocouple K, respectively. Both parameters were simultaneously recorded through a data acquisitor connected to a PC. Heating rates of 5, 7, 10, and 14 °C/min were used under a normal atmosphere.

Results and discussion

Analysis of TG data

The mass losses of both samples determined at different heating rates were situated between 350 and 850 °C for sample C and between 500 and 1000 °C for sample G. From these data the degree of conversion was calculated using the following expression:

$$\alpha = \frac{W_S - w(t,T)}{W_S - W_F} \quad (10)$$

where W_S is the initial mass, W_F is the final mass, and $w_{(t,T)}$ is the instantaneous mass depending on both the time and the temperature. The curve of conversion versus the temperature is shown in Fig. 1.

These experimental curves were fitted by a sigmoidal function to calculate both $d\alpha/dT$ and $d^2\alpha/dT^2$ data. The first derivative $d\alpha/dT$ versus T obtained at different β is shown in Fig. 2.

From these data the peak temperature (T_P), the corresponding conversion (α_{max}), and the peak conversion rates $(d\alpha/dt)_{max}$ were determined by each heating rate. The values of these parameters are listed in Table 2.

The T_P represents the temperature at which the maximum rate of mass loss occur. From Fig. 2 and Table 2 it is observed that in both samples T_P moves to higher temperatures and $(d\alpha/dt)_{max}$ increases in intensity when the heating rate increases. Under similar heating conditions fairly higher values of peak conversion rates are observed in powder C. This means that a higher decomposition rate is occurring in the powder with petroleum coke addition.

In both samples it is noted that the maximum reaction rate is obtained at a constant degree of decomposition ($\alpha_{max} \cong 0.50$) independently of the heating rate.

Energy activation of sample C

The plots $\ln\beta$ versus $1/T_\alpha$ (OFW method) and $\ln(\beta/T_\alpha^2)$ versus $1/T_\alpha$ (KAS method) at different heating rates

Table 1 Chemical composition (wt%) of the mold flux

SiO_2	CaO	MgO	Al_2O_3	MnO	TiO_2	Fe_2O_3	Na_2O	K_2O	F	P_2O_5
36.2	30.8	2.1	5.1	0.1	0.2	1.6	12.7	0.7	10.4	0.1

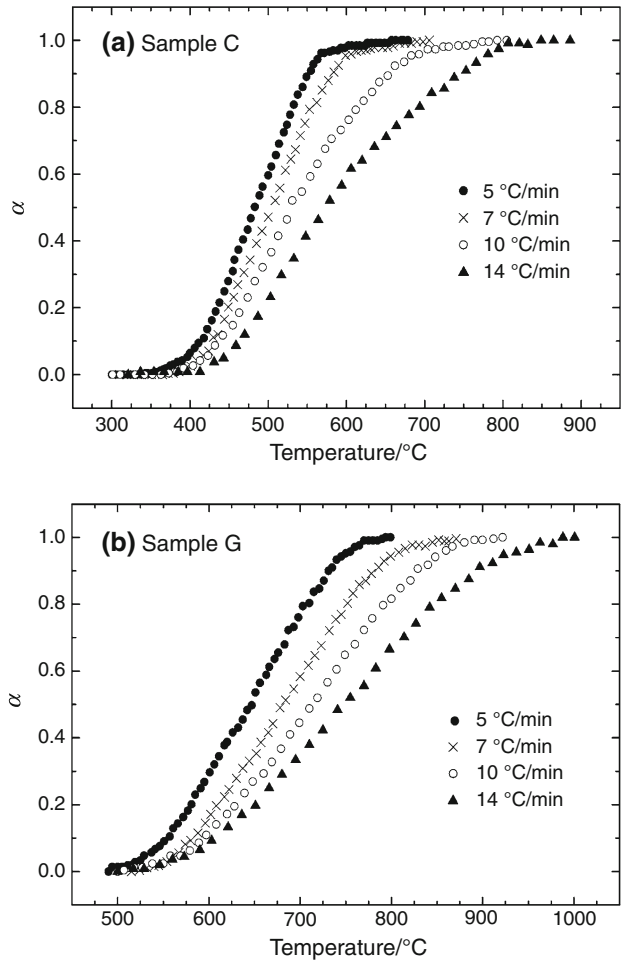

Fig. 1 Degree of conversion (α) curves for different heating rates corresponding to **a** powder C, and **b** powder G

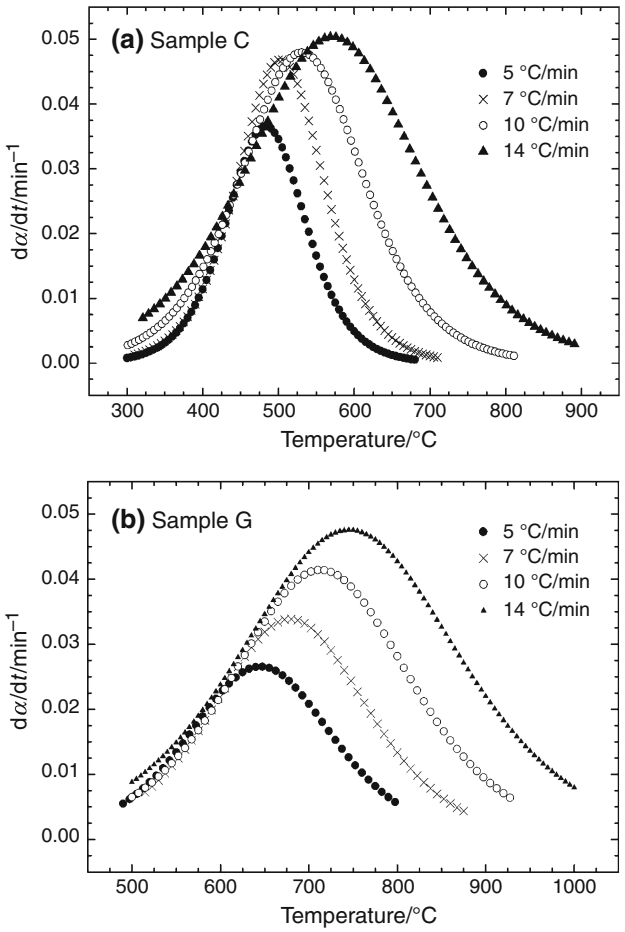

Fig. 2 Conversion rate versus temperature plots for different heating rates for **a** sample C, and **b** sample G

corresponding to mold powder with 15 wt% coke are shown in Fig. 3. From the slopes of these straight lines the activation energies of decomposition at different degree of conversion were calculated.

The E values calculated for sample C at different degrees of decomposition (α) and their correlation coefficients (R^2) are indicated in Table 3. From these R^2 values it is observed that the best fitting ocurrs at a degree of conversion between 0.3 and 0.7.

In both models the activation energy of the sample with petroleum coke decreases when the degree of decomposition increases. Hence, non constant E values would be indicating the occurrence of different decomposition phenomena.

The mean value of E obtained from OFW and KAS methods was E_{coke} (OFW) = 54.0 kJ/mol and E_{coke} (KAS) = 43.1 kJ/mol, respectively.

Plots of $\ln(\beta/T_P^2)$ versus $1/T_P$ (Fig. 4a) and $\ln(\beta/(T_P - T_0))$ versus $1/T_P$ (Fig. 4b) were built to calculate the activation energy using Kissinger and Augis–Bennet methods, respectively.

From these curves, the activation energy corresponding to sample C was: E_{coke} (Kissinger) = 46.7 kJ/mol ($R^2 = 0.95019$), and E_{coke} (Augis–Bennet) = 49.2 kJ/mol ($R^2 = 0.95938$).

Both methods present similar values of activation energy with correlation coefficients R^2 higher than 0.95. These values of E are in good correspondence with mean values of E calculated by the OFW and KAS methods.

Energy activation of sample G

The same methods were used to evaluate E values of sample G (mold flux with 15 wt% synthetic graphite). In Fig. 5, the plots of $\ln\beta$ versus $1/T_\alpha$ (OFW method, Fig. 5a) and $\ln(\beta/T_\alpha^2)$ versus $1/T_\alpha$ (KAS method, Fig. 5b) are observed.

Table 4 shows the energy activation corresponding to sample with 15% graphite obtained at different percentage of decomposition α. From R^2 values it is observed that the best fittings are situated between 0.3 and 0.95.

Similarly to sample C, the activation energy of sample G decreases when the degree of decomposition increases.

Table 2 Values of T_P, α_{max}, and $(d\alpha/dt)_{max}$ for decomposition process of samples at different rates

Sample C				Sample G			
β/°C min^{-1}	TP/°C	α_{max}	$(d\alpha/dt)_{max}$/min^{-1}	β/°C min^{-1}	T_P/°C	α_{max}	$(d\alpha/dt)_{max}$/min^{-1}
5	483	0.50	0.0366	5	645	0.50	0.0266
7	502	0.48	0.0469	7	678	0.49	0.0339
10	531	0.50	0.0480	10	713	0.50	0.0414
14	571	0.49	0.0504	14	745	0.48	0.0476

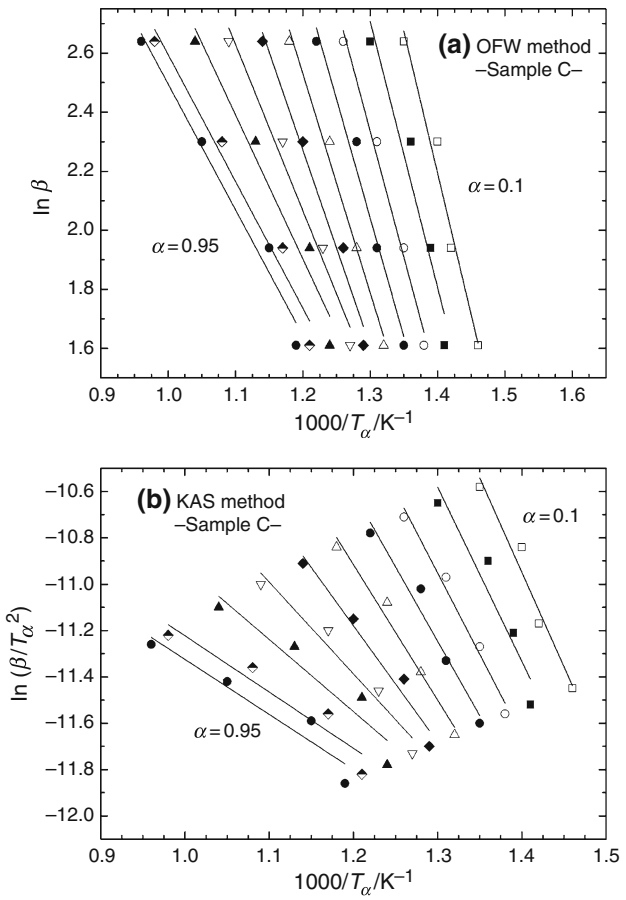

Fig. 3 Curves of fitting using **a** OFW and **b** KAS methods applied to different conversion of mold powder with 15 wt% petroleum coke

However, in the powder with graphite the activation energy shows an almost constant value at different α values between 0.4 and 0.9, indicating that a single reaction mechanism is actuating in this interval of α.

From OFW and KAS methods the mean value of the activation energy was: $E_{graphite}$ (OFW) = 77.2 kJ/mol and $E_{graphite}$ (KAS) = 63.2 kJ/mol, respectively.

The plots built to obtain the activation energy from Kissinger and Augis–Bennet methods are present in Fig. 6.

The activation energy determined by Kissinger and Augis–Bennet methods was: $E_{graphite}$ (Kissinger) = 61.5 kJ/mol ($R^2 = 0.99286$), and $E_{graphite}$ (Augis–Bennet) = 65.8 kJ/mol ($R^2 = 0.99393$).

Table 3 Activation energy (E) and correlation coefficients (R^2) obtained at different conversion (α) of sample C

α	Sample C—OFW method		Sample C—KAS method	
	E/kJ mol^{-1}	R^2	E/kJ mol^{-1}	R^2
0.1	76.0	0.95893	67.7	0.94156
0.2	71.2	0.91061	62.5	0.87007
0.3	67.4	0.98326	58.4	0.97243
0.4	63.6	0.96760	53.4	0.94823
0.5	58.6	0.98280	48.6	0.96938
0.6	52.5	0.97414	41.8	0.94981
0.7	44.5	0.96986	32.9	0.93313
0.8	38.5	0.94478	25.9	0.85175
0.9	33.9	0.95822	20.2	0.86237
0.95	33.7	0.96538	19.7	0.87236

Similarly to sample C, both methods present similar values of E and R^2. Comparing the correlation coefficients obtained with these two methods, sample G shows a higher precision on the fitting of slopes ($R^2 > 0.99$) than sample C ($R^2 > 0.95$).

Taken into account the activation energy obtained by the four methods, it is possible to assign a value of $E \approx 48$ kJ/mol to sample C and $E \approx 67$ kJ/mol to sample G. Thus, the mold powder with 15 wt% coke is the least thermally stable material.

Considering the design of a mold powder, the lower activation energy corresponding to the powder with coke translates into higher reactivity of this powder respect to the sample with graphite.

On the other hand, the XRD diffraction pattern of the coke sample showed only one broad peak, between $2\theta = 20$–30°, corresponding to a type of fully amorphous carbon. For synthetic graphite the peaks corresponding to only one crystalline phase: graphite (main peak in $2\theta = 26.6^\circ$) was found. Thus, synthetic graphite exhibits a greater order of crystallinity than petroleum coke. By this, because the reactivity of carbonaceous materials depends on the graphitization degree of carbon crystals, the XRD

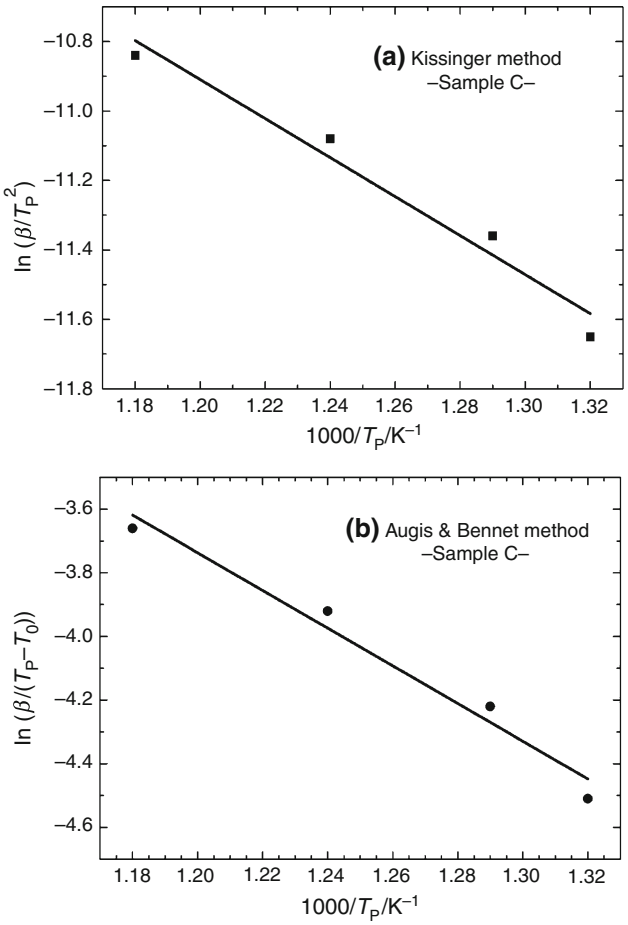

Fig. 4 Plots to calculate E values corresponding to sample with 15 wt% coke from **a** Kissinger, and **b** Augis–Bennet methods

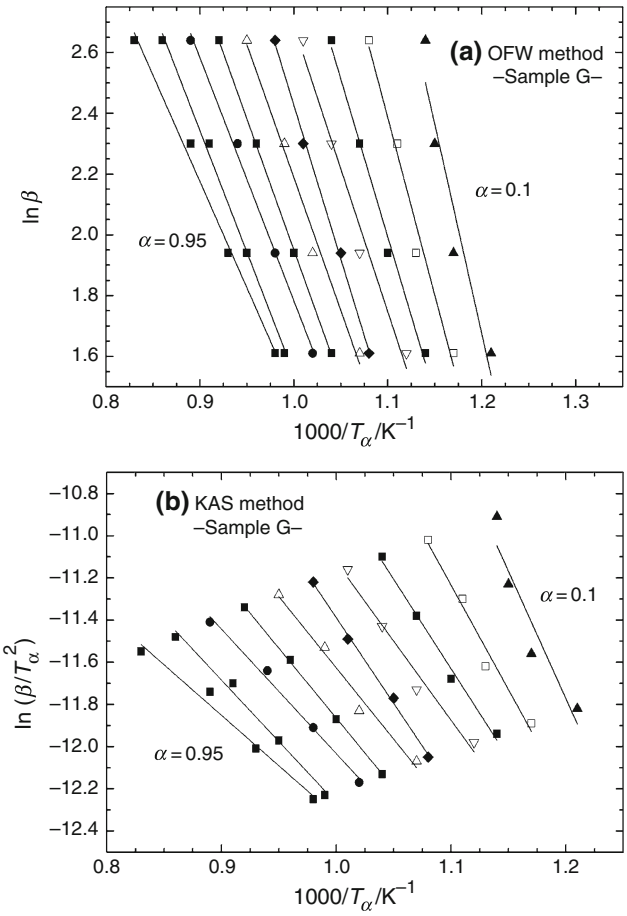

Fig. 5 Fitting curves using **a** OFW and **b** KAS methods applied to different conversion of mold powder with 15 wt% synthetic graphite

suggests that petroleum coke should be more reactive than synthetic graphite. This fact is in accord with the E results obtained in the decomposition analysis of both carbonaceous samples.

Order of reaction

The selected interval used to calculate the order of reaction n, Eq. 9, was 450–525 °C for sample C and 600–725 °C for sample C. The temperatures and the conversion degrees at these temperatures $\alpha(T)$ are listed in Table 5.

Using these α and β values in Eq. 9, Fig. 7 is obtained. A linear fitting is performed for each temperature and from the slopes of the straight lines the n values are recorded and listed in Table 6.

Figure 7 denotes a very good fitting of experimental data. The n values for sample C are in the range 1.0–1.4, while for sample G this range is narrower: 1.2–1.3.

Taking into account experimental errors and approximations inherent to the model, it is suggested that the decomposition process of both carbonaceous samples develops with an order of reaction equal to the unity.

Table 4 Activation energy (E) and correlation coefficients (R^2) obtained at different conversion (α) of sample G

α	Sample G—OFW method		Sample G—KAS method	
	E/kJ mol^{-1}	R^2	E/kJ mol^{-1}	R^2
0.1	108.8	0.87271	100.3	0.83835
0.2	97.1	0.96918	82.3	0.96288
0.3	92.3	0.98879	70.5	0.98561
0.4	74.3	0.96762	62.4	0.96046
0.5	80.0	0.99700	67.5	0.99535
0.6	69.2	0.98153	56.2	0.97289
0.7	68.2	0.99962	55.1	0.99936
0.8	63.2	0.99477	49.0	0.98810
0.9	63.2	0.99477	48.4	0.98527
0.95	55.3	0.98917	39.8	0.97001

Mold powder with synthetic graphite addition (sample G) presented a more constant value of both n and E than one with petroleum coke (sample C). This fact would be indicating that the degradation process for sample C is more complex than for sample G. If several reactions are

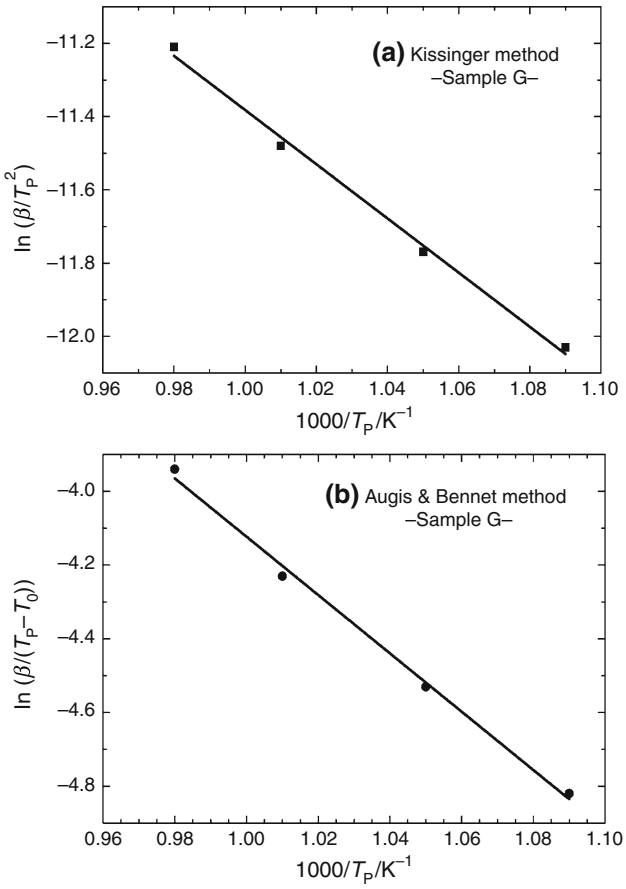

Fig. 6 Plots to calculate E values corresponding to sample with 15 wt% graphite from **a** Kissinger, and **b** Augis–Bennet methods

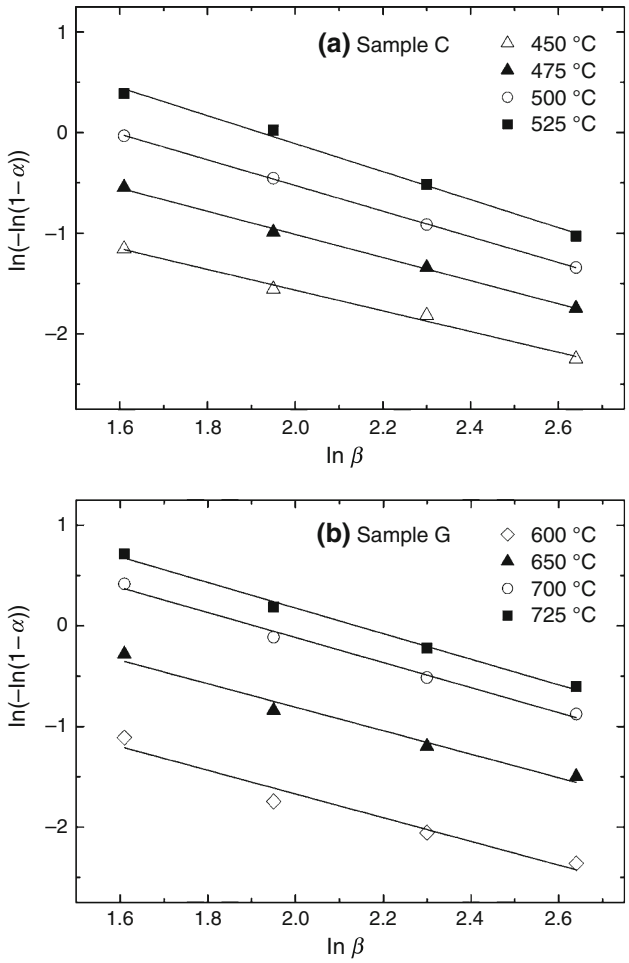

Fig. 7 Curves of fitting to calculate the reaction order n of **a** sample C, and **b** sample G, at different β

Table 5 Conversion (α) obtained for the same temperature at different heating rates

Sample C	β/°C min^{-1}	450 °C	475 °C	500 °C	525 °C
	5	0.27	0.44	0.62	0.77
	7	019	0.31	0.47	0.64
	10	0.15	0.23	0.33	0.45
	14	0.10	0.16	0.23	0.30
Sample G	β/°C min^{-1}	600 °C	650 °C	700 °C	725 °C
	5	0.28	0.53	0.78	0.87
	7	0.16	0.35	0.59	0.70
	10	0.12	0.26	0.45	0.55
	14	0.09	0.20	0.34	0.42

concurrent, it may be assumed that each one contributes with its own E value. For example, the decomposition activation energy of asphaltite varied with the conversion degree [31]. This variation was attributed to parallel reactions occurring in same conditions during its pyrolysis process [31].

Table 6 Order of reaction (n) and correlation coefficients (R^2) as a function of temperature for samples C and G

Sample C			Sample G		
T/°C	n	R^2	T/°C	n	R^2
450	1.03	0.9860	600	1.18	0.9422
475	1.15	0.9963	650	1.16	0.9663
500	1.28	0.9998	700	1.24	0.9877
525	1.39	0.9907	725	1.27	0.9908

In both cases, the decomposition reaction of carbonaceous materials depends on both thermodynamic and kinetic considerations. The kinetic considerations begin when the gas penetrates the carbonaceous particles. The decomposition reaction depends on several simultaneous processes when the reactioning interface moves inward. The rate of reaction can be limited by the rate of reactant diffusion inward, the rate of product diffusion outward, or the chemical reaction rate at the interface. Thus, the

decrease of E when the reaction increase could also be due to the particle size distribution presents in both carbonaceous materials. Because the rate of decomposition increase when the particle size decrease [32], the first reactioning particles would be the finest one. So, firstly the fine particles react with O_2 producing CO/CO_2 (gas) and they start to open the powder structure. Then, when the reaction grade (α) progress, the gas produced by decomposition of greater particles of carbonaceous materials finds a more open interparticle path. So, a lower activation energy would be present when the degree of conversion progress due to increased rate of product diffusion (CO and/or CO_2) outward. Thus, the reactivity of carbonaceous material into the mold powder can be also somewhat controlled by selecting an adequate particle size distribution.

Conclusions

A good correspondence of the activation energy of decomposition applying four non-isothermal methods was attained. From these models the average activation energy corresponding to mold flux with 15 wt% of coke ($E = 48$ kJ/mol) was lower than one with 15 wt% of graphite ($E = 67$ kJ/mol). Besides, a first order of reaction ($n = 1$) was assumed for the decomposition kinetic of both types of carbonaceous materials.

The lower activation energy corresponding to the powder with coke was translated into higher reactivity of this powder respect to the sample with graphite. This fact would be considered during the mold powder design because it has an important influence on its melting rate.

From the variation of E and n values with conversion degree and temperature, it was observed that the powder with petroleum coke showed a less thermally stable behavior and a more complex degradation process. Both aspects would be taken into account during the formation of intermediate sintered layer (rich in carbon) because it protects the steel surface from oxidation.

References

1. Mills KC, Fox AB, Li Z, Thackray RP. Performance and properties of mould fluxes. Ironmak Steelmak. 2005;32:26–34.
2. Branion RV. Mold fluxes for continuous casting. Iron Steelmak. 1986;13:41–50.
3. Pinheiro CA, Samarasekera IV, Brimacombe JK. Mold flux for continuous casting of steel. Iron Steelmak. 1995;22:43–4.
4. Mahapatra RB, Brimacombe JK, Samarasekera IV. Mold behavior and its influence on quality in the continuous casting of steel slabs: Part II. Mold heat transfer, formation of oscillation marks, longitudinal off-corner depressions, and subsurface cracks. Mater Trans B. 1991;22:875–88.
5. Brandaleze E, Santini L, Gorosurreta C, Benavidez E, Martin A. Influence of carbonaceous particles on the melting behaviour of mold fluxes at high temperature. Proceedings 16th Steelmaking Conference IAS. San Nicolás, Argentina 2007. pp. 363–71.
6. Kawamoto M, Nakajima K, Kanazawa T, Nakai K. Design principles of mold powder for high speed continuous casting. ISIJ Int. 1994;34:593–8.
7. Wei E, Yang Y, Feng C, Sommerville ID, McLean A. Effect of carbon properties on melting behavior of mold fluxes for continuous casting of steels. J Iron Steel Res. 2006;13:22–6.
8. Chrissafis K. Kinetics of thermal degradation of polymers. J Therm Anal Calorim. 2009;95:273–83.
9. Sánchez-Jiménez PE, Criado JM, Pérez-Maqueda LA. Kissinger kinetic analysis of data obtained under different heating schedules. J Therm Anal Calorim. 2008;94:427–32.
10. Silva AR, Crespi MS, Ribeiro CA, Oliveira SC, Silva MRS. Kinetic of thermal decomposition of residues from different kinds of composting. J Therm Anal Calorim. 2004;75:401–9.
11. Choudhury D, Borah RC, Goswamee RL, Sharmah HP, Rao PG. Non-isothermal thermogravimetric pyrolysis kinetics of waste petroleum refinary sludge by isoconversional approach. J Therm Anal Calorim. 2007;89:965–70.
12. Jablonski AE, Lang AJ, Vyazovkin S. Isoconversional kinetics of degradation of polyvinylpyrrolidone used as a matrix for ammonium nitrate stabilization. Thermochim Acta. 2008;474:78–80.
13. Rodante F, Vecchio S, Tomassetti M. Multi-step decomposition processes for some antibiotics: a kinetic study. Thermochim Acta. 2002;394:7–18.
14. Küçük F, Yildiz K. The decomposition kinetics of mechanically activated alunite ore in air atmosphere by thermogravimetry. Thermochim Acta. 2006;448:107–10.
15. Bernardo da Cruz AG, Wardell JL, Rocco AM. The decomposition kinetics of [Et4N]2[M(dmit)2] (M = Ni, Pd) in a nitrogen atmosphere using thermogravimetry. Thermochim Acta. 2006;443:217–24.
16. Otero M, Gómez X, Garcia AI, Moran A. Non-isothermal thermogravimetric analysis of the combustion of two different carbonaceus materials. J Therm Anal Calorim. 2008;93:619–26.
17. Goncalves MLA, da Pinto Mota DA, Teixeira AMRF, Teixeira MAG. Pyrolysis of petroleum fractions. J Therm Anal Calorim. 2008;91:341–6.
18. Vlase T, Vlase G, Birta N, Doca N. Comparative results of kinetic data obtained with different methods for complex decomposition steps. J Therm Anal Calorim. 2007;88:631–5.
19. De Angelis Curtis S, Kurdzie K, Materazzi S, Vecchio S. Crystal structure and thermoanalytical study of a manganese(II) complex with 1-allylimidazole. J Therm Anal Calorim. 2008;92:109–14.
20. Kropidłowska A, Rotaru A, Strankowski M, Becker B, Segal E. Heteroleptic cadmium(II) complex, potential precursor for semiconducting CDS layers. J Therm Anal Calorim. 2008;91:903–9.
21. Pielichowski K, Świerz-Motysia B. Influence of polyesterurethane plasticizer on the kinetics of poly(vinyl chloride) decomposition process. J Therm Anal Calorim. 2006;83:207–12.
22. Boonchom B. Kinetic and thermodynamic studies of $MgHPO_4 \cdot 3H_2O$ by non-isothermal decomposition data. J Therm Anal Calorim. 2009;98:863–71.
23. Vlase G, Vlase T, Tudose R, Costişor O, Doca N. Kinetic of decomposition of some complexes under non-isothermal conditions. J Therm Anal Calorim. 2007;88:637–40.
24. Santhosh G, Cheng Tien RP, Ghee AH. Thermal decomposition kinetics of ammonium dinitramide–guanylurea dinitramide mixture analyzed by isoconversional methods. Thermochim Acta. 2008;480:43–8.

25. Ozawa T. A new method of analyzing thermogravimetric data. Bull Chem Soc Jpn. 1965;38:1881–6.
26. Flynn JH, Wall LA. A quick, direct method for the determination of activation energy from thermogravimetric data. Polym Lett. 1966;4:323–8.
27. Kissinger HE. Reaction kinetics in differential thermal analysis. Anal Chem. 1957;29:1702–6.
28. Akahira T, Sunose T. Measurement to decide a factor of thermal life on insulating materials. Rep Chiba Inst Technol. 1971;16: 22–31.
29. Augis JA, Bennet JA. Calculation of the Avrami parameters for heterogeneous solid state reactions using a modification of the Kissinger method. J Therm Anal. 1978;13:283–92.
30. Ozawa T. Kinetics of non-isothermal crystallization. Polymer. 1971;12:150–8.
31. Tonbul Y, Saydut A, Yurdakoc K, Hamamci C. A kinetic investigation on the pyrolysis of Seguruk asphaltite. J Therm Anal Calorim. 2009;95:197–202.
32. Zamalloa M, Ma D, Utigard TA. Oxidation rates of industrial cokes with CO_2 and air. ISIJ Int. 1995;35:458–63.